Electronic Supplementary Information for:

Fundamental and overtone vibrational spectroscopy, enthalpy of hydrogen bond formation and equilibrium constant determination of the methanol-dimethylamine complex

*Lin Du, Kasper Mackeprang, and Henrik G. Kjaergaard**

Department of Chemistry, University of Copenhagen, Universitetsparken 5, DK-2100

Copenhagen Ø, Denmark

*Corresponding author:

Email: hgk@chem.ku.dk

FAX: 45-35320322

Phone: 45-35320334

May 2, 2013

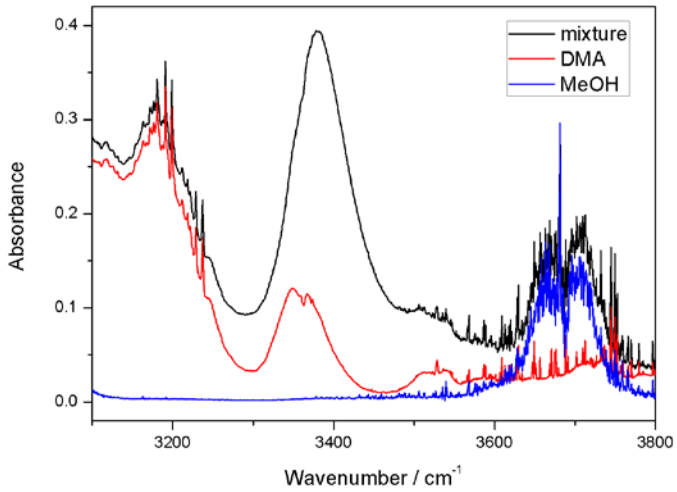

Figure S1. Spectra of 466 Torr DMA, 25 Torr MeOH, and a mixture of the two gases recorded with a 10 cm path length cell with MIR light source and MCT detector at 301 K.

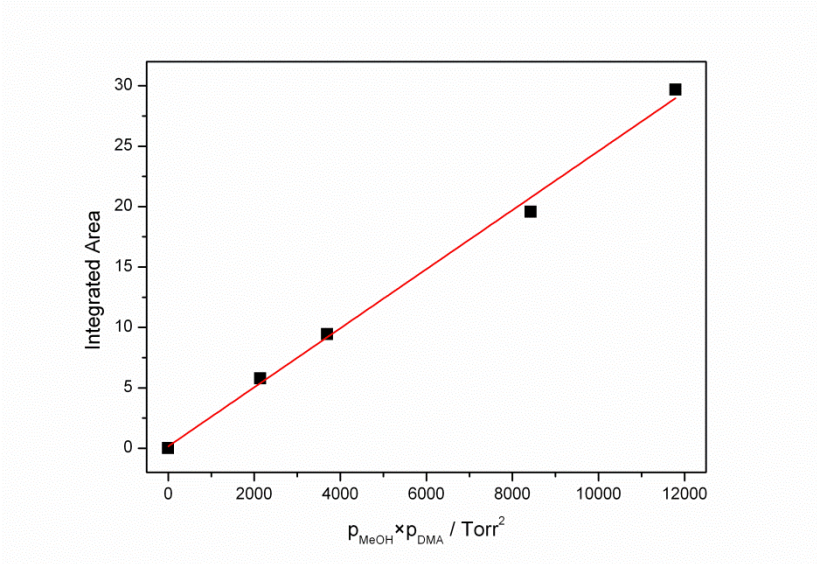

Figure S2. The integrated absorbance of the OH-stretching band in MeOH-DMA complex as a function of the product of the MeOH and DMA pressures. The band was integrated in the range between 3100 and 3640 cm^{-1}.

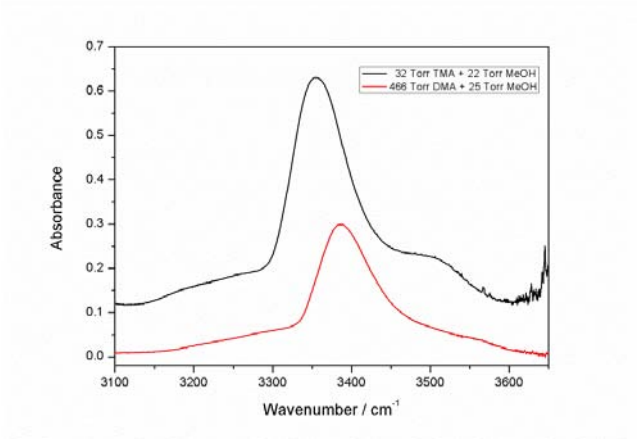

Figure S3. The $\tilde{\nu}_{OH}$ transition of the MeOH-DMA complex obtained by spectral subtraction of 466 Torr DMA and 25 Torr MeOH from the mixture of the two gases (black), and of the MeOH-TMA complex obtained by spectral subtraction of 32 Torr TMA and 22 Torr MeOH from the mixture of the two gases (red). The MeOH-DMA spectrum was recorded with a 10 cm path length cell at 300 K and the MeOH-TMA spectrum was recorded with a 2.4 m path length cell at 298 K. The MeOH-TMA spectrum is offset by 0.1 absorbance unit to avoid overlapping between the spectra.

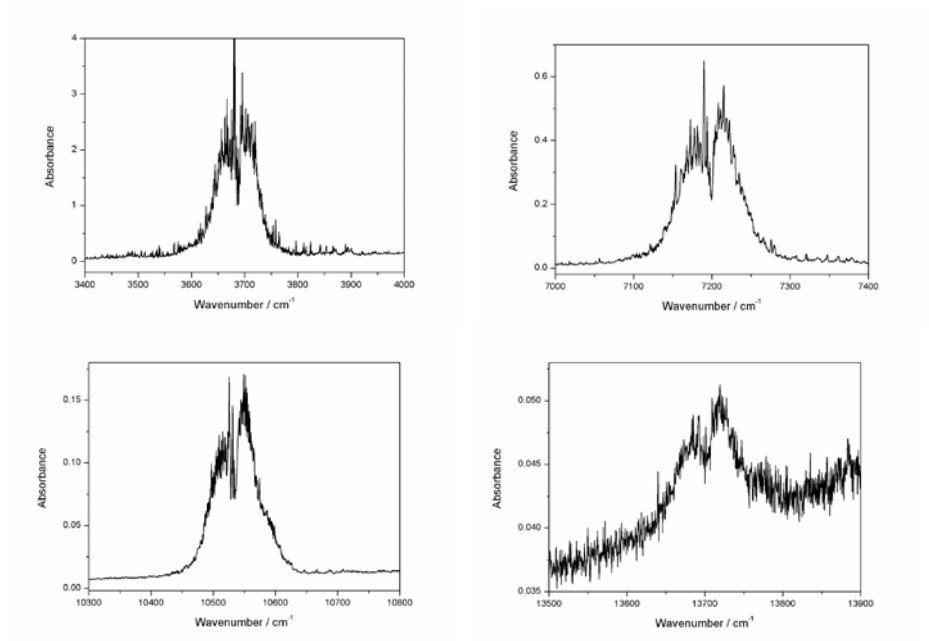

Figure S4. The room temperature (298 K) vapor phase overtone spectra of MeOH in the Δv_{OH} = 1 – 4 regions. The Δv_{OH} = 1 and 2 spectra were recorded at a pressure of 22 Torr and a pathlength of 2.4 m with MCT detector and MIR light source. The Δv_{OH} = 3 and 4 spectra were recorded at a pressure of 64 Torr and a path length of 4.8 m with InGaAs detector and NIR light source.

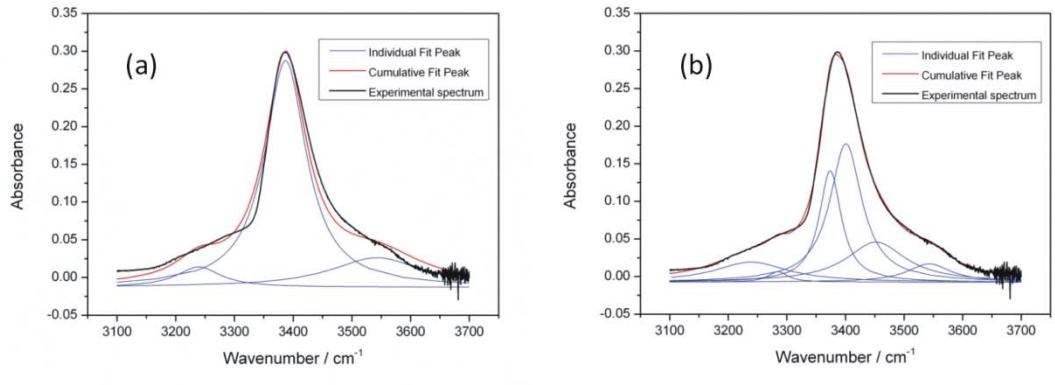

Figure S5. The deconvolution fitting of the OH-stretching fundamental transition band of MeOH-DMA: (a) three-band fitting; (b) six-band fitting.

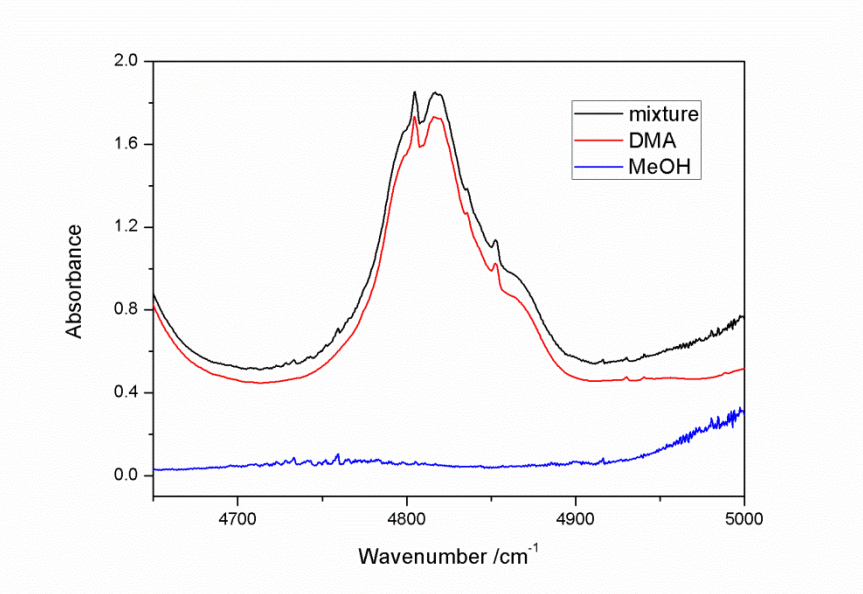

Figure S6. Spectra of 202 Torr DMA, 36 Torr MeOH, and a mixture of the two gases recorded in a 4.8 m path length cell with NIR light source and InGaAs detector at 297 K. The two upper spectra are offset by 0.3 to avoid overlapping between the spectra.

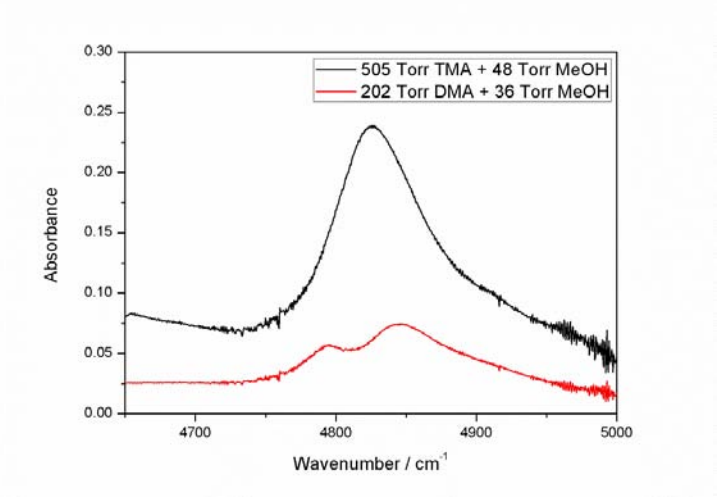

Figure S7. The $\tilde{\nu}_{OH} + \delta_{COH}$ bands of the MeOH-TMA complex obtained by spectral subtraction of 505 Torr TMA and 48 Torr MeOH from the mixture of the two gases (black) and of the MeOH-DMA complex obtained by spectral subtraction of 202 Torr DMA and 36 Torr MeOH from the mixture of the two gases (red). Both spectra were recorded with NIR light source and InGaAs detector in a 4.8 m path length cell.

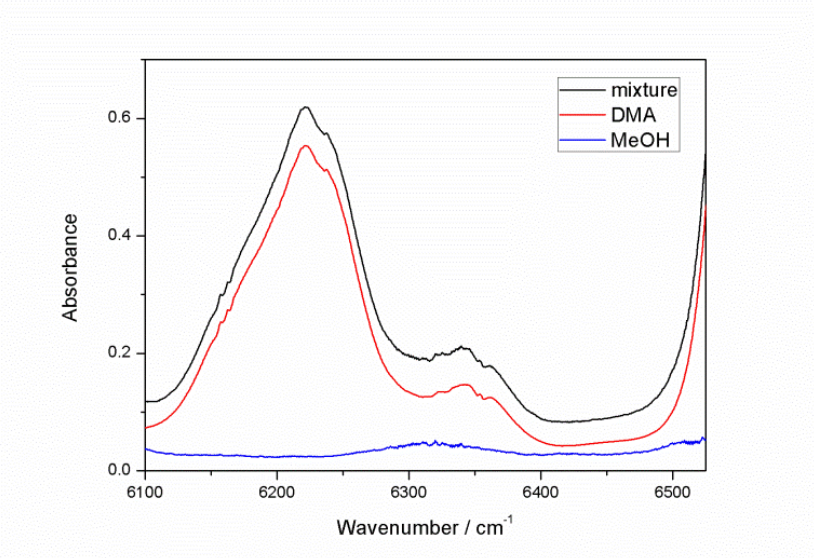

Figure S8. Spectra of 146 Torr DMA, 48 Torr MeOH, and a mixture of the two gases recorded in a 4.8 m path length cell with NIR light source and InGaAs detector at 300 K.

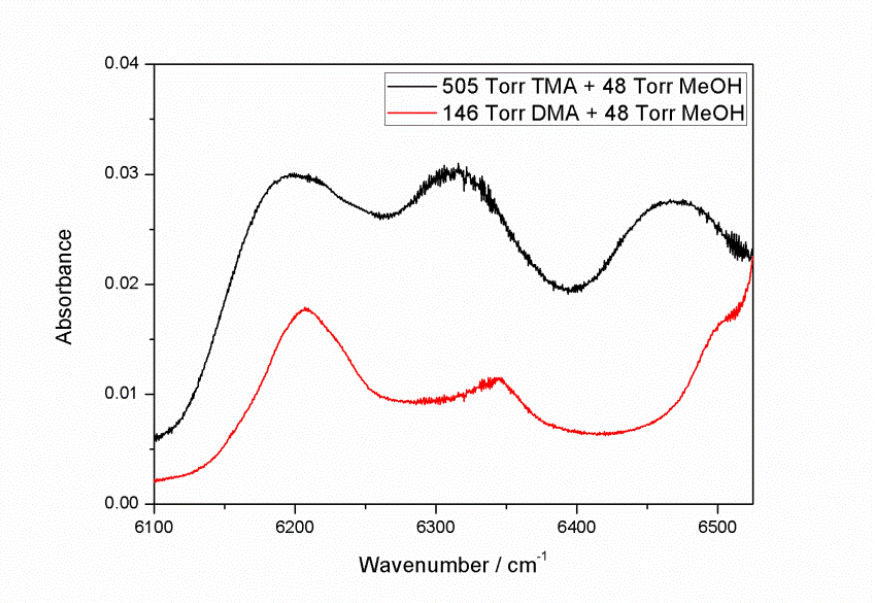

Figure S9. The $2\tilde{\nu}_{OH}$ bands of the MeOH-TMA complex obtained by spectral subtraction of 505 Torr TMA and 48 Torr MeOH from the mixture of the two gases (black) and of the MeOH-DMA complex obtained by spectral subtraction of 146 Torr DMA and 48 Torr MeOH from the mixture of the two gases (red). Both spectra were recorded in a 4.8 m path length cell with NIR light source and InGaAs detector.

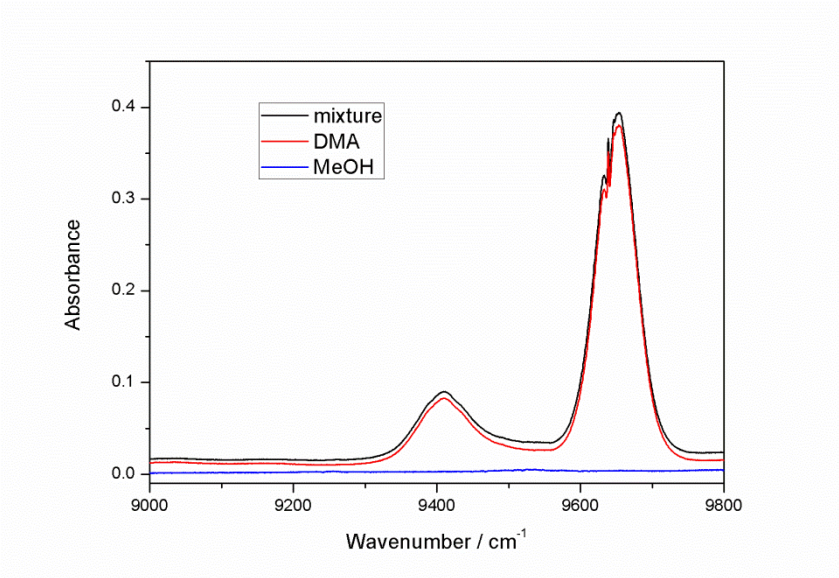

Figure S10. Spectra of 202 Torr DMA, 36 Torr MeOH, and a mixture of the two gases recorded with a 4.8 m path length cell with NIR light source and InGaAs detector at 297 K.

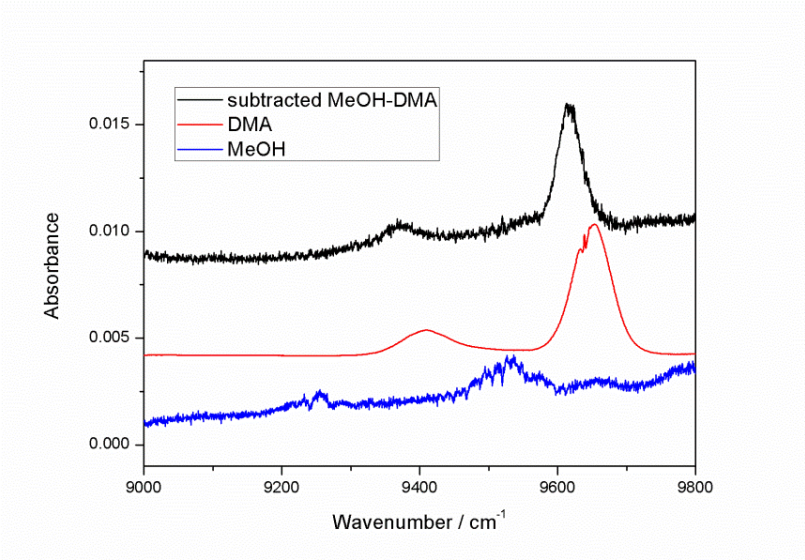

Figure S11. Spectra of DMA, MeOH and the MeOH-DMA complex in the 9000-9800 cm^{-1} region. The DMA spectrum was scaled down 60 times to show it at a scale comparable with the other two spectra.

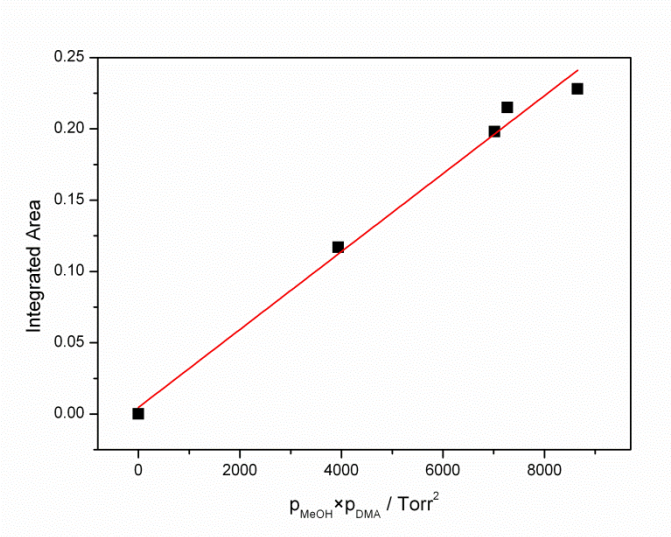

Figure S12. The integrated absorbance of the NH-stretching second overtone band ($3\tilde{\nu}_{NH}$) in the MeOH-DMA complex as a function of the product of the MeOH and DMA pressures. The band was integrated in the range between 9568 and 9672 cm^{-1}.

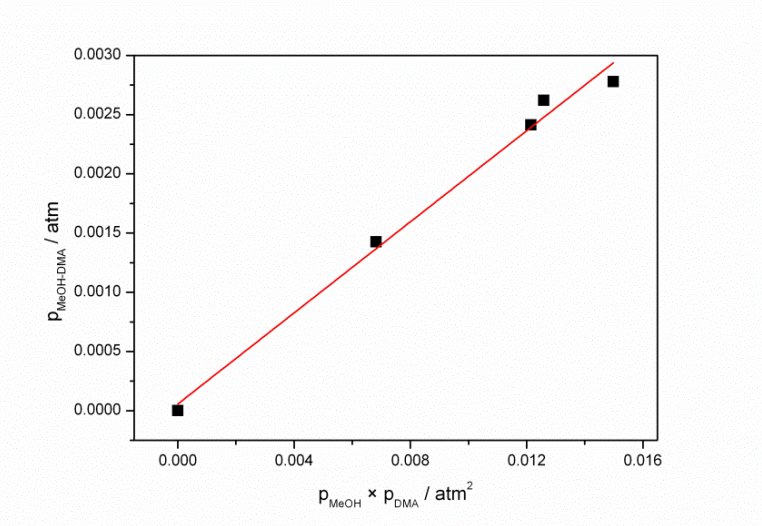

Figure S13. Plot of $p_{MeOH\text{-}DMA}$ against $p_{MeOH} \times p_{DMA}$. The $p_{MeOH\text{-}DMA}$ values are derived from the measured $3\tilde{\nu}_{NH}$ overtone absorbance and the local mode calculated intensity.

Table S1. Calculated frequencies and IR intensities for MeOH-DMA (A, B, C) with harmonic oscillator at the B3LYP/aug-cc-pVTZ level

MeOH-DMA (A)		MeOH-DMA (B)		MeOH-DMA (C)	
$\tilde{\nu}$ / cm^{-1}	I / km mol^{-1}	$\tilde{\nu}$ / cm^{-1}	I / km mol^{-1}	$\tilde{\nu}$ / cm^{-1}	I / km mol^{-1}
9	5.0279	11	6.4806	27	2.9533
50	0.6971	45	0.3204	41	6.4776
64	1.4530	52	2.3396	42	3.8786
109	1.0602	110	1.1215	66	18.0855
118	2.2927	157	1.2503	91	3.9419
195	0.5747	170	0.5718	136	0.5773
221	0.0575	225	0.0614	229	0.0545
281	3.4443	276	2.7093	264	2.1969
391	5.2223	393	6.6054	291	94.7843
763	48.1618	772	50.2676	386	3.5270
845	117.5028	828	137.8728	830	135.9724
931	2.5677	933	1.9241	951	0.2659
1035	10.2047	1035	11.3136	1033	112.9842
1068	95.2421	1068	87.7042	1040	6.8050
1095	0.8858	1096	0.4694	1075	8.5656
1134	8.3007	1135	6.4523	1101	0.0254
1155	27.8471	1157	27.4748	1168	33.7315
1171	0.7691	1171	0.7390	1173	1.2119
1200	10.0463	1200	10.6395	1185	10.2283
1267	0.1041	1267	0.1647	1266	0.7094
1445	0.6902	1444	0.5307	1364	21.4001
1467	40.2879	1464	30.5136	1440	1.5332
1470	1.5000	1470	1.1912	1466	0.6819
1473	9.5637	1475	3.2315	1478	1.1652
1476	0.1906	1476	0.0809	1480	4.3596
1490	5.1219	1489	3.2750	1494	9.9383
1497	3.7456	1498	1.8931	1496	5.4866
1500	10.9857	1500	17.0093	1504	1.0456
1513	3.4786	1512	4.6602	1508	4.5707
1515	12.8494	1516	11.9862	1516	1.0149
1517	3.0447	1518	2.1966	1533	8.1306
2962	70.3483	2961	37.8943	2915	51.1022
2963	179.3322	2962	169.0096	2918	189.2260
2966	44.0852	2967	73.3516	3001	65.1324
2999	72.7948	3001	70.6563	3033	61.4599
3061	22.9591	3058	35.6193	3034	24.3359
3064	17.0317	3059	12.6574	3051	44.4335
3081	53.1565	3081	53.3942	3086	28.9361
3101	20.6353	3102	16.0361	3086	35.6422
3106	18.7182	3102	23.2928	3120	10.0363
3453	956.2803	3466	942.2122	3517	79.3748
3514	3.3007	3511	6.6107	3831	33.0146

Table S2. Calculated frequencies and IR intensities for MeOH, DMA, and MeOH-TMA with harmonic oscillator at the B3LYP/aug-cc-pVTZ level

MeOH		DMA		MeOH-TMA	
$\tilde{\nu}$ / cm^{-1}	I / km mol^{-1}	$\tilde{\nu}$ / cm^{-1}	I / km mol^{-1}	$\tilde{\nu}$ / cm^{-1}	I / km mol^{-1}
291	105.3523	229	0.0912	18	5.8042
1039	120.8185	257	2.1990	46	0.5247
1076	1.5007	381	5.8392	47	1.4360
1171	0.4291	755	106.8981	111	1.1559
1366	24.5451	935	4.2519	116	1.7105
1477	3.1561	1035	8.7188	173	0.3534
1498	2.9741	1100	0.0553	244	0.0023
1509	5.3599	1165	32.2985	265	0.3522
2994	62.9849	1184	7.6051	266	0.3911
3040	53.2719	1266	0.1464	393	23.7369
3108	24.3408	1442	1.7993	418	0.1801
3829	31.0260	1467	0.7200	420	0.1811
		1476	4.8496	778	44.5244
		1488	2.6902	824	42.2208
		1495	11.5421	1043	16.9104
		1516	3.0269	1046	23.0806
		1517	12.7969	1067	94.0080
		2925	49.4240	1069	0.0295
		2928	162.8559	1117	2.7260
		3043	45.0389	1120	6.8887
		3043	23.4796	1136	8.9626
		3090	25.6822	1171	0.7246
		3090	31.6898	1221	23.4539
		3527	0.5624	1294	8.1802
				1297	9.5904
				1443	1.6541
				1443	0.0678
				1464	34.3574
				1476	0.0352
				1483	0.0498
				1486	5.6106
				1488	11.3159
				1489	0.0834
				1498	1.8777
				1506	28.4378
				1512	10.9841
				1512	12.3036
				1514	0.5153
				2933	37.9221
				2935	38.6991
				2944	237.6115
				2967	76.2153
				3001	68.3845
				3061	18.6580
				3063	27.2497
				3068	18.8441
				3082	54.4627
				3101	4.8682
				3104	30.4236
				3109	23.8998
				3448	1005.1270

Table S3. Calculated binding energies (BE), zero point vibrational energy (ZPVE) corrected binding energies, enthalpies of formation (ΔH_{298K}), Gibbs free energies of formation (ΔG_{298K}) and equilibrium constant (K_p) at 298 K for MeOH-DMA (B) [a]

	B3LYP/ aug-cc-pVTZ	LC-wPBE/ aug-cc-pVTZ	M06-2X/ aug-cc-pVTZ	wB97XD/ aug-cc-pVTZ	CCSD(T)-F12a/ VDZ-F12
BE	-26.3	-26.9	-33.0	-35.3	-33.4
BE(ZPVE)	-20.5	-21.2	-27.4	-29.1	
BE(ZPVE)[b]	-27.5	-27.7	-27.8	-27.2	
ΔH_{298K}	-19.5	-20.1	-26.7	-28.5	
ΔH_{298K}[b]	-26.6	-26.7	-27.1	-26.6	
ΔG_{298K}	11.0	9.2	8.9	6.1	
ΔG_{298K}[b]	4.0	2.7	8.5	8.0	
K_p	1.2×10^{-2}	2.4×10^{-2}	2.7×10^{-2}	8.7×10^{-2}	
K_p[b]	2.0×10^{-1}	3.4×10^{-1}	3.2×10^{-2}	4.0×10^{-2}	

[a] All energies given in kJ mol^{-1}, and all K_p given in atm^{-1}. [b] Calculated with the CCSD(T)-F12a/VDZ-F12 optimized electronic energies and the DFT thermal correction.

Table S4. Calculated binding energies (BE), zero point vibrational energy (ZPVE) corrected binding energies, enthalpies of formation (ΔH_{298K}), Gibbs free energies of formation (ΔG_{298K}) and equilibrium constant (K_p) at 298 K for MeOH-DMA (C) [a]

	B3LYP/ aug-cc-pVTZ	LC-wPBE/ aug-cc-pVTZ	M06-2X/ aug-cc-pVTZ	wB97XD/ aug-cc-pVTZ	CCSD(T)-F12a/ VDZ-F12
BE	-9.5	-9.7	-17.0	-15.8	-16.4
BE(ZPVE)	-6.4	-6.6	-12.5	-12.3	
BE(ZPVE)[b]	-13.3	-13.4	-11.9	-12.9	
ΔH_{298K}	-3.8	-4.1	-11.1	-10.1	
ΔH_{298K}[b]	-10.7	-10.8	-10.5	-10.8	
ΔG_{298K}	23.1	22.8	24.5	20.6	
ΔG_{298K}[b]	16.2	16.1	25.1	19.9	
K_p	9.0×10^{-5}	1.0×10^{-4}	5.0×10^{-5}	2.5×10^{-4}	
K_p[b]	1.5×10^{-3}	1.5×10^{-3}	4.0×10^{-5}	3.3×10^{-4}	

[a] All energies given in kJ mol^{-1}, and all K_p given in atm^{-1}. [b] Calculated with the CCSD(T)-F12a/VDZ-F12 optimized electronic energies and the DFT thermal correction.

Table S5. Calculated binding energies (BE), zero point vibrational energy (ZPVE) corrected binding energies, enthalpies of formation (ΔH_{298K}), Gibbs free energies of formation (ΔG_{298K}) and equilibrium constant (K_p) at 298 K for MeOH-MeOH [a]

	B3LYP/ aug-cc-pVTZ	LC-wPBE/ aug-cc-pVTZ	M06-2X/ aug-cc-pVTZ	wB97XD/ aug-cc-pVTZ	CCSD(T)-F12a/ VDZ-F12
BE	-19.8	-19.3	-24.9	-23.8	-24.4
BE(ZPVE)	-14.5	-14.2	-19.5	-18.7	
BE(ZPVE)[b]	-19.1	-19.3	-19.0	-19.3	
ΔH_{298K}	-13.3	-12.9	-18.7	-17.4	
ΔH_{298K}[b]	-17.9	-18.0	-18.2	-18.0	
ΔG_{298K}	15.5	14.8	14.7	9.2	
ΔG_{298K}[b]	10.9	9.8	15.2	8.7	
K_p	2.0×10^{-3}	2.5×10^{-3}	2.7×10^{-3}	2.4×10^{-2}	
K_p[b]	1.2×10^{-2}	2.0×10^{-2}	2.2×10^{-3}	3.1×10^{-2}	

[a] All energies given in kJ mol^{-1}, and all K_p given in atm^{-1}. [b] Calculated with the CCSD(T)-F12a/VDZ-F12 optimized electronic energies and the DFT thermal correction.

Table S6. Calculated OH- and NH-stretching wavenumbers and intensities of the MeOH-DMA complex (conformer B) with the anharmonic oscillator local mode method at CCSD(T)-F12a/VDZ-F12 level

Δv	OH_b				NH_f			
	$\tilde{\nu}$ /cm^{-1}	$\Delta\tilde{\nu}$ /cm^{-1} [a]	f_{OHb}	f_{OHb}/f_M	$\tilde{\nu}$ /cm^{-1}	$\Delta\tilde{\nu}$ /cm^{-1} [b]	f_{NHf}	f_{NHf}/f_M
1	3290	403	1.8×10^{-4}	48.9	3378	4	1.2×10^{-7}	2.2
2	6334	879	7.6×10^{-8}	0.1	6604	7	3.6×10^{-7}	1.0
3	9133	1427	1.6×10^{-8}	0.7	9677	7	1.8×10^{-8}	0.8
4	11686	2047	1.1×10^{-9}	0.8	12598	7	9.0×10^{-10}	0.8
5	13995	2739	3.0×10^{-10}	2.8	15367	4	6.1×10^{-11}	0.8

[a] $\Delta\tilde{\nu} = \tilde{\nu}_{MeOH} - \tilde{\nu}_{OHb.}$ [b] $\Delta\tilde{\nu} = \tilde{\nu}_{DMA} - \tilde{\nu}_{NHf.}$

Table S7. Calculated OH- and NH-stretching wavenumbers and intensities of the MeOH-DMA complex (conformer C) with the anharmonic oscillator local mode method at CCSD(T)-F12a/VDZ-F12 level

Δv	OH_f				NH_b			
	$\tilde{\nu}$ /cm^{-1}	$\Delta\tilde{\nu}$ /cm^{-1} [a]	f_{OHf}	f_{OHf}/f_M	$\tilde{\nu}$ /cm^{-1}	$\Delta\tilde{\nu}$ /cm^{-1} [b]	f_{NHb}	f_{NHb}/f_M
1	3694	-1	3.5×10^{-6}	1.0	3379	3	1.2×10^{-5}	224
2	7216	-3	6.1×10^{-7}	1.0	6609	2	6.8×10^{-8}	0.2
3	10564	-5	2.2×10^{-8}	0.9	9689	-4	9.0×10^{-9}	0.4
4	13740	-7	1.3×10^{-9}	0.9	12618	-13	9.5×10^{-10}	0.9
5	16743	-10	8.3×10^{-11}	0.8	15398	-26	8.3×10^{-11}	1.1

[a] $\Delta\tilde{\nu} = \tilde{\nu}_{MeOH} - \tilde{\nu}_{OHf.}$ [b] $\Delta\tilde{\nu} = \tilde{\nu}_{DMA} - \tilde{\nu}_{NHb.}$

Table S8. Calculated OH_b- and OH_f- stretching wavenumbers and intensities of the MeOH-MeOH complex with the anharmonic oscillator local mode method at CCSD(T)-F12a/VDZ-F12 level

Δv_{OH}	OH_b				OH_f			
	$\tilde{\nu}$ /cm^{-1}	$\Delta\tilde{\nu}$ /cm^{-1} [a]	f_{OHb}	f_{OHb}/f_M	$\tilde{\nu}$ /cm^{-1}	$\Delta\tilde{\nu}$ /cm^{-1} [b]	f_{OHf}	f_{OHf}/f_M
1	3543	150	9.0×10^{-5}	25.1	3692	1	5.8×10^{-6}	1.6
2	6892	321	3.6×10^{-8}	0.1	7213	0	6.1×10^{-7}	1.0
3	10047	512	4.9×10^{-9}	0.2	10562	-3	2.1×10^{-8}	0.9
4	13008	725	1.3×10^{-9}	0.9	13739	-6	1.1×10^{-9}	0.8
5	15776	958	1.9×10^{-10}	1.7	16745	-11	1.1×10^{-10}	1.0

[a] $\Delta\tilde{\nu} = \tilde{\nu}_{MeOH} - \tilde{\nu}_{OHb.}$ [b] $\Delta\tilde{\nu} = \tilde{\nu}_{MeOH} - \tilde{\nu}_{OHf.}$

Table S9. Calculated harmonic OH- and NH-stretching wavenumbers and intensity (oscillator strength) of MeOH, DMA and MeOH-DMA (A) with various DFT methods

		B3LYP/ aug-cc-pVTZ	LC-wPBE/ aug-cc-pVTZ	M06-2X/ aug-cc-pVTZ	wB97XD/ aug-cc-pVTZ
OH in MeOH	$\tilde{\nu}$ / cm^{-1}	3829	3920	3901	3918
	f	5.8×10^{-6}	8.6×10^{-6}	8.5×10^{-6}	6.4×10^{-6}
NH in DMA	$\tilde{\nu}$ / cm^{-1}	3527	3620	3563	3582
	f	1.1×10^{-7}	7.2×10^{-7}	4.4×10^{-7}	1.6×10^{-7}
OH in MeOH-DMA	$\tilde{\nu}$ / cm^{-1}	3453	3522	3529	3542
	f	1.8×10^{-4}	1.8×10^{-4}	1.5×10^{-4}	1.6×10^{-4}
	$\Delta\tilde{\nu}_{OH}$/ cm^{-1} [a]	376	398	372	376
NH in MeOH-DMA	$\tilde{\nu}$ / cm^{-1}	3514	3608	3567	3579
	f	6.2×10^{-7}	1.3×10^{-6}	1.9×10^{-6}	1.6×10^{-6}
	$\Delta\tilde{\nu}_{NH}$/ cm^{-1} [b]	13	12	-4	3

[a] $\Delta\tilde{\nu}_{OH} = \tilde{\nu}_{MeOH} - \tilde{\nu}_{MeOH\text{-}DMA}$. [b] $\Delta\tilde{\nu}_{NH} = \tilde{\nu}_{DMA} - \tilde{\nu}_{MeOH\text{-}DMA}$.

Table S10. Experimental details for MeOH-DMA measurements

Transition	p_{DMA} / Torr	p_{MeOH} / Torr	Path length / m	Integrated absorbance/ cm^{-1}	T / K
$\tilde{\nu}_{OH}$	466	25	0.1	37.539	301
	229	37	0.1	25.892	298
	231	16	0.1	11.167	299
	131	17	0.1	6.717	299
	64	22	2.4	78.795	298
	64	22	2.4	62.036	308
	64	22	2.4	41.649	318
	64	22	2.4	26.132	328
	64	22	2.4	17.814	338
	64	22	2.4	11.748	348
	64	22	2.4	7.208	358
$2\tilde{\nu}_{OH}$	146	48	4.8	-	300
$2\tilde{\nu}_{NH}$	27	27	4.8	0.865	297
$3\tilde{\nu}_{NH}$	202	36	4.8	0.215	297
	151	26	4.8	0.117	297
	146	48	4.8	0.198	297
	258	34	4.8	0.228	297

Table S11. Experimental details for MeOH-TMA measurements

Transition	p_{TMA} / Torr	p_{MeOH} / Torr	Path length / m	Integrated absorbance/ cm^{-1}	T / K
$\tilde{\nu}_{OH}$	32	22	2.4	54.298	298
	32	22	2.4	40.173	308
	32	22	2.4	24.793	318
	32	22	2.4	16.566	328
	32	22	2.4	10.702	338
	32	22	2.4	6.700	348
	32	22	2.4	4.207	358
$2\tilde{\nu}_{OH}$	505	48	4.8	-	300

Table S12. Calculated dipole moment functions and potential energy surfaces for OH- and NH-displacement in MeOH, DMA and MeOH-DMA (A) at CCSD(T)-F12a/VDZ-F12 level

OH-displacement in MeOH				
Δr / Å	dx / Debye	dy / Debye	dz / Debye	Energy / Hartree
-0.30	0.0	1.50377416	0.71335021	-115.4017891
-0.25	0.0	1.47803597	0.76328603	-115.4791085
-0.20	0.0	1.45498276	0.81231908	-115.5302985
-0.15	0.0	1.43456071	0.85981205	-115.5628099
-0.10	0.0	1.41675751	0.90498058	-115.5819315
-0.05	0.0	1.40158256	0.94694981	-115.5914638
0.00	0.0	1.38906548	0.98479909	-115.5941599
0.05	0.0	1.37925488	1.01756989	-115.5920240
0.10	0.0	1.37221266	1.04429131	-115.5865217
0.15	0.0	1.36800483	1.06399783	-115.5787307
0.20	0.0	1.36669105	1.07576604	-115.5694474
0.25	0.0	1.36831005	1.07873697	-115.5592620
0.30	0.0	1.37289043	1.07215807	-115.5486133

NH-displacement in DMA				
Δr / Å	dx / Debye	dy / Debye	dz / Debye	Energy / Hartree
-0.30	0.90278012	0.0	-0.58244063	-134.8272144
-0.25	0.92046358	0.0	-0.55667524	-134.8859049
-0.20	0.93634926	0.0	-0.53474130	-134.9255210
-0.15	0.94995410	0.0	-0.51690507	-134.9511310
-0.10	0.96071444	0.0	-0.50354238	-134.9664404
-0.05	0.96802362	0.0	-0.49508919	-134.9741856
0.00	0.97126357	0.0	-0.49200014	-134.9764034
0.05	0.96982874	0.0	-0.49472320	-134.9746179
0.10	0.96314660	0.0	-0.50368062	-134.9699732
0.15	0.95070409	0.0	-0.51924965	-134.9633315
0.20	0.93207693	0.0	-0.54173583	-134.9553450
0.25	0.90693886	0.0	-0.57134715	-134.9465081
0.30	0.87511181	0.0	-0.60815492	-134.9371970

OH-displacement in MeOH-DMA (A)				
Δr / Å	dx / Debye	dy / Debye	dz / Debye	Energy / Hartree
-0.30	0.50709724	-2.15820719	-0.27815815	-250.4146883
-0.25	0.59472091	-2.22446044	-0.24181232	-250.4829997
-0.20	0.69068164	-2.29962532	-0.20272744	-250.5280137
-0.15	0.79684048	-2.38506335	-0.16011907	-250.556408
-0.10	0.91524612	-2.48229016	-0.11312843	-250.5729545
-0.05	1.04814308	-2.59299048	-0.06082226	-250.5811057
0.00	1.19791332	-2.71899491	-0.00221938	-250.5833796
0.05	1.36696426	-2.86217722	0.06366331	-250.581625
0.10	1.55756716	-3.024331	0.13774658	-250.577208
0.15	1.77167279	-3.20699835	0.22080805	-250.5711445
0.20	2.01060838	-3.41128368	0.31339206	-250.5641928
0.25	2.27497336	-3.6377088	0.41574163	-250.5569179
0.30	2.56442511	-3.88599632	0.52767971	-250.5497373

NH-displacement in MeOH-DMA (A)				
Δr / Å	dx / Debye	dy / Debye	dz / Debye	Energy / Hartree
-0.30	1.23777789	-2.60198246	0.05466894	-250.4344191
-0.25	1.22682069	-2.62962805	0.04027043	-250.4930099
-0.20	1.21758302	-2.65477876	0.02762606	-250.532563
-0.15	1.2100568	-2.67693487	0.01686788	-250.558136
-0.10	1.20425391	-2.69547942	0.00817259	-250.5734261
-0.05	1.20019733	-2.70973315	0.00174061	-250.5811634
0.00	1.19791332	-2.71899492	-0.00221937	-250.5833796
0.05	1.19742716	-2.72256957	-0.00350103	-250.5815946
0.10	1.19875883	-2.7197918	-0.0019096	-250.576949
0.15	1.20191853	-2.71005374	0.00272811	-250.570302
0.20	1.2068975	-2.6928313	0.01055045	-250.5623031
0.25	1.21366858	-2.66773536	0.02165196	-250.5534447
0.30	1.22217469	-2.63446715	0.03606976	-250.5441007

Z-matrix of MeOH-DMA (A) at CCSD(T)-F12a/VDZ-F12 level:

```
N
C  1 B1
H  2 B2  1 A1
H  2 B3  1 A2  3 D1
H  2 B4  1 A3  3 D2
C  1 B1  2 A4  4 D3
H  6 B3   1 A2   2 -D3
H  6 B2   1 A1   2 D5
H  6 B4   1 A3   2 D6
C  1 B9   6 A8   2 D7
H 10 B10  1 A9   6 D8
H 10 B11  1 A10  6 D9
H 10 B11  1 A10  6 D10
O 10 B13  1 A12  6 D8
H 14 B14 10 A13  1 0.0
H  1 B15  6 A14  2 D13

B1       1.4624208
B2       1.0908377
A1     108.7506659
B3       1.0893354
A2     109.6647197
D1     117.9638996
B4       1.0975724
A3     112.9012376
D2    -120.3004988
A4     111.5642148
D3    -175.8141072
D5     -66.2216003
D6      54.0785716
B9       3.7060914
A8     109.9477958
D7     122.2523780
B10      1.0892476
A9     150.8702139
D8     -61.6630721
B11      1.0955512
A10     88.2144416
D9      64.0944540
D10    172.5794458
B13      1.4126943
A12     43.1391182
B14      0.9746422
A13    107.9841474
B15      1.0123184
A14    109.1621146
D13   -120.7275321
```